

# Journal of the Air & Waste Management Association



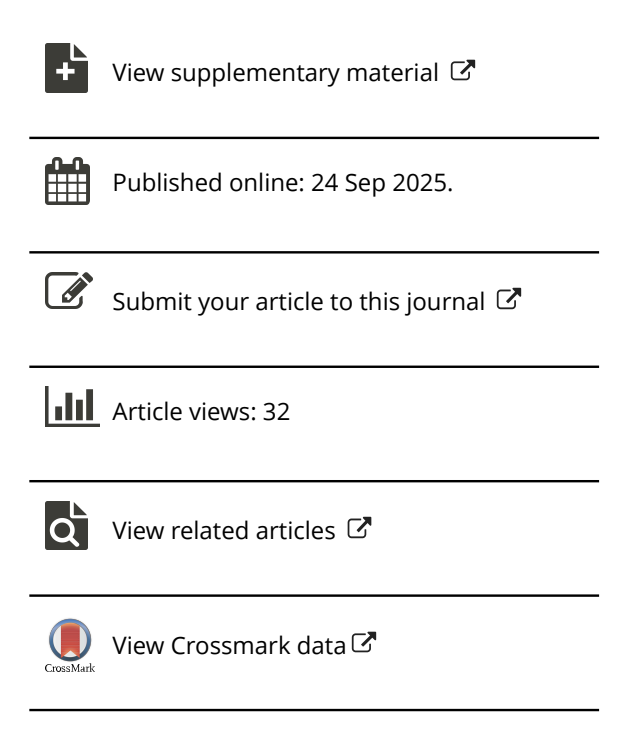
ISSN: 1096-2247 (Print) 2162-2906 (Online) Journal homepage: www.tandfonline.com/journals/uawm20

# High-resolution analysis of seasonal spatial variation for urban air pollution: Implications for exposure assessment

Sooyoung Guak, Jaehoon An, Dong-Hyun Lee, Wonho Yang, Jusung Park & Kiyoung Lee

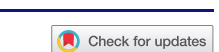
**To cite this article:** Sooyoung Guak, Jaehoon An, Dong-Hyun Lee, Wonho Yang, Jusung Park & Kiyoung Lee (24 Sep 2025): High-resolution analysis of seasonal spatial variation for urban air pollution: Implications for exposure assessment, Journal of the Air & Waste Management Association, DOI: 10.1080/10962247.2025.2552978

To link to this article: <a href="https://doi.org/10.1080/10962247.2025.2552978">https://doi.org/10.1080/10962247.2025.2552978</a>





#### **TECHNICAL PAPER**



# High-resolution analysis of seasonal spatial variation for urban air pollution: Implications for exposure assessment

Sooyoung Guak<sup>a,b</sup>, Jaehoon An<sup>c</sup>, Dong-Hyun Lee<sup>d</sup>, Wonho Yang<sup>e</sup>, Jusung Park<sup>f</sup>, and Kiyoung Lee<sup>a,b</sup>

<sup>a</sup>Department of Environmental Health Sciences, Graduate School of Public Health, Seoul National University, Seoul, Korea; <sup>b</sup>Institute of Health and Environment, Seoul National University, Seoul, Korea; <sup>c</sup>Department of Health Sciences, Graduate School of Public Health, Seoul National University, Seoul, Korea; <sup>d</sup>Consulting & Technology for Environment Health Safety, Seoul, Korea; <sup>e</sup>Department of Occupational Health, Daegu Catholic University, Gyeongsan-si, Korea; <sup>f</sup>Seoul Metropolitan Government Research Institute of Public Health and Environment, Gwacheon-si, Korea

#### **ABSTRACT**

Exposure to air pollutants is associated with significant health effects. Accurate exposure assessment remains a critical yet challenging aspect of environmental health research. Although air quality monitoring station (AQMS) data are commonly used as a surrogate for personal exposure, diverse spatial-temporal variations can lead to significant exposure misclassification. This study aimed to identify the seasonal spatial variation of five air pollutants (PM<sub>2.5</sub>, PM<sub>10</sub>, NO<sub>2</sub>, CO, and O<sub>3</sub>) at city and small spatial scales (1 km<sup>2</sup>) in Seoul, Korea, using data from the AQMSs and in-situ monitoring sites (IMSs) for high-resolution measurements. Measurements were conducted across four seasons over one year, covering city-, district-, and small-scale spatial units, with a detailed focus on a 1 km<sup>2</sup> area within one administrative district. The air pollutant concentrations were obtained from the 25 AQMSs in each district. Fine-scale measurements were carried out at eight IMSs within a 1 km<sup>2</sup> area surrounding a single AQMS in Guro-gu, Seoul. To enable direct comparison, measurements from the AQMS and IMS were simultaneously collected following standard monitoring protocols. Moran's index was used as an indicator of spatial autocorrelation to identify the homogeneity and heterogeneity of air pollutants by spatial units. Concentrations of pollutants at IMSs were overall higher than those at nearby the AQMS, except for  $O_3$  concentrations in the spring and summer. Seasonal spatial autocorrelation patterns in city-scale areas did not reflect variations in small-scale areas. These findings highlight the limitations of relying solely on AQMS data for exposure assessment and underscore the value of integrating high-resolution data to reduce estimation errors. This study provides a framework for enhancing air quality management and exposure assessment strategies by accounting for spatial-temporal variations, especially in areas lacking dense monitoring networks.

Implications: This study integrates city-scale air quality monitoring station (AQMS) data with high-resolution in-situ measurements to reveal discrepancies in seasonal spatial patterns of air pollutants across different spatial scales in Seoul, Korea. By directly comparing AQMS and IMS data using standard monitoring methods, it demonstrates that commonly used AQMS-based exposure estimates may significantly underestimate pollution levels in small-scale urban environments. This high-resolution approach highlights the critical need for incorporating fine-scale monitoring to improve personal exposure assessment in areas with sparse monitoring coverage.

#### **PAPER HISTORY**

Received April 16, 2025 Revised August 19, 2025 Accepted August 22, 2025

# Introduction

Air pollutant concentrations are monitored by the national air quality monitoring station (AQMS). Exposure to air pollutants has been linked to increased adverse health effects (Cohen et al. 2017; Costa et al. 2017; Mills et al. 2015; Sørhaug et al. 2006). Epidemiological studies have often used air pollutant concentrations at AQMSs as a surrogate for personal exposure because of the limited resources for direct measurements (Atkinson et al. 2013; Chen et al. 2018). However, this approach may underestimate health risks, as combined indoor and outdoor

PM<sub>2.5</sub> exposure has been associated with higher mortality risk than outdoor exposure alone (Dong et al. 2020). This can lead to estimation errors due to diverse spatial-temporal variations of air pollutants. While high-resolution ambient measurements alone cannot fully represent personal exposure, they can help reduce exposure misclassification—particularly in unmonitored or heterogeneous urban areas—by providing improved area-level estimates for exposure modeling and epidemiological studies.

To mitigate estimation errors in air pollution levels in unmonitored areas, it is essential to account for spatialtemporal variations of air pollutants. Previous studies have reported that the spatial-temporal variation of air pollutants differs across spatial scales. On a regional scale, many studies in China reported spatial-temporal variations in areas >100,000 km<sup>2</sup> at a regional scale (Hu et al. 2014; Yang and Christakos 2015; Zhao et al. 2013). On a city-scale, spatial-temporal distributions were reported in Beijing (Chen, Tang, and Zhao 2015; Ji, Wang, and Zhuang 2019; Xu et al. 2019) and Guangzhou, China (Li et al. 2014); Vancouver (Marshall, Nethery, and Brauer 2008), and Toronto, Canada (Su et al. 2010); Ankara, Turkey (Raja et al. 2018); and Kaunas, Lithuania (Dėdelė and Miškinytė 2019). Air pollutant concentrations can be easily affected by climatic conditions, traffic intensity, population density, and the distance from the sources (Merbitz, Fritz, and Schneider 2012). In smaller areas, it is possible to identify high spatial-temporal variation, including the effects of these factors, more accurately. In exposure assessment, the interpolation method, dispersion model, and land use regression model are commonly used to estimate personal exposure to air pollutants by accounting for high spatial resolution in unmonitored areas (Arunachalam et al. 2014; Hoek et al. 2008).

The Korean government has disclosed the hourly concentrations of criteria air pollutants, including particulate matter with an aerodynamic diameter of  $\leq 2.5 \,\mu \text{m}$  and  $\leq 10 \,\mu \text{m}$  (PM<sub>2.5</sub> and PM<sub>10</sub>, respectively), nitrogen dioxide (NO<sub>2</sub>), carbon monoxide (CO), sulfur dioxide (SO<sub>2</sub>), ozone (O<sub>3</sub>), lead, and benzene at the AQMSs. Air quality in Seoul, with an area of 605.4 km<sup>2</sup>, is monitored by 25 AQMSs. Seoul consists of 25 administrative districts referred to as "gu"; each gu has one urban AQMS. However, data from a single AQMS in each gu may not be sufficient to estimate air pollution in that area. An additional AQMS is operated at 15 roadside air quality monitoring networks using vehicles equipped with standard monitoring methods that are the same as the AQMS. These mobile monitoring methodologies were easily applied to obtain air quality data with high spatial resolution (Tessum et al. 2018). Determining spatial-temporal variations in the unmonitored areas of each gu is useful to estimate air pollutant exposure.

The aim of this study was to identify seasonal spatial variation of five air pollutants ( $PM_{2.5}$ ,  $PM_{10}$ ,  $NO_2$ , CO, and  $O_3$ ) at the city-scale using 25 AQMSs and small-scale areas ( $1 \text{ km}^2$ ) at one of the 25 administrative districts in Seoul, Korea. In this study, the spatial–temporal variation of air pollutants was identified at a city-scale and smaller spatial scales in Seoul, Korea, over one year. Spatial units were compared with standard monitoring methods in city-, district-, and small-scale areas.

#### **Materials and methods**

# Study area

Seoul, with an area of 605.4 km², consists of 25 administrative districts referred to "gu." Each of 25 districts operates one urban AQMS to monitor ambient air quality in Seoul. An additional AQMS is operated at 15 roadside air quality monitoring networks using vehicles equipped with standard monitoring methods, the same as AQMS. The area of each gu ranges from 10–47 km². The population of Seoul was 9,638,799 in 2023, and each gu had a population in the range of 131,793–660,025 (https://kosis.kr/index/index.do). The population per area of each gu in Seoul ranged from 6,292–25,244 people per km².

Guro-gu, with an area of 20.12 km<sup>2</sup>, is one of the 25 gu in Seoul and had a population of 415,651 in 2023 (https://kosis.kr/index/index.do). The population per area of Guro-gu was 20,659 people per km<sup>2</sup>. The testbed area for small-scale measurement was chosen based on both practical and scientific considerations. Initially, a  $5 \times 5 \text{ km}^2$  area centered on the existing urban AQMS in Guro-gu was designated. Grid cells outside the administrative boundary of Guro-gu were excluded to ensure consistency within a single jurisdiction, and eight in-situ monitoring sites (IMSs) were finally selected. The total of eight IMSs, each with an area of 1 km<sup>2</sup>, in thr test-bed area were selected to measure the air quality for un-monitored areas in Guro-gu. The locations of the 25 AQMSs and eight IMSs in Seoul are shown in Figure 1. The geographical coordinates of monitoring sites in Seoul are shown in Table S1. The characteristics of the eight IMSs differed. Location 1 was in the vicinity of the highway, and thus had high traffic intensity. Location 2 was in the vicinity of a liquefied petroleum gas charge station. Location 3 was near a train station (Guro station). Location 4 was in a residential area nearby a barbeque restaurant and parking lot. Location 5 was in a park (Guro Geori park). Location 6 was in a residential area in the vicinity of a restaurant that utilized charcoal. Location 7 was in a large parking lot of the Korea University Hospital. Location 8 was in a predominantly business area.

# Air pollutant concentrations

The air quality data of five criteria air pollutants (PM<sub>2.5</sub>, PM<sub>10</sub>, NO<sub>2</sub>, CO, and O<sub>3</sub>) were monitored by 25 AQMSs and eight IMSs in Seoul from December 2017–December 2018. The sampling periods were classified into winter (December 2017–February 2018), spring (March–June 2018), summer

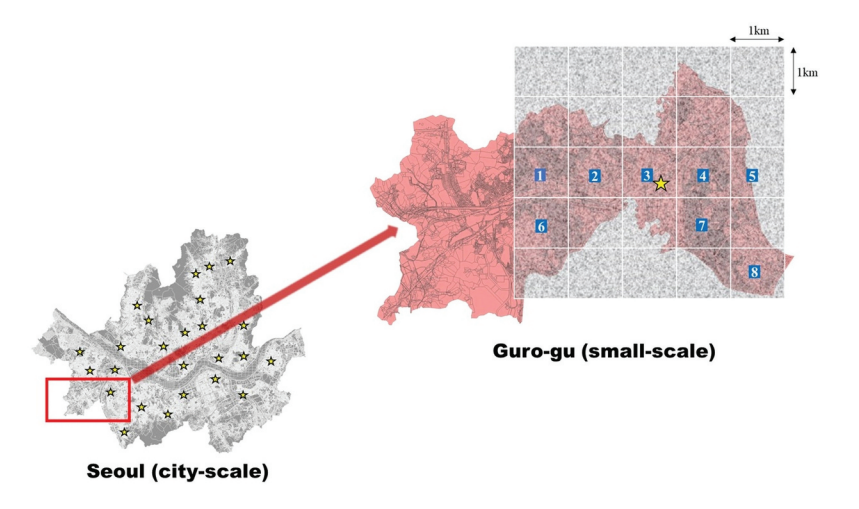


**Figure 1.** Locations of monitoring sites in Seoul. Yellow stars represent air quality monitoring stations (AQMSs) and blue squares represent in-situ monitoring sites (IMSs).

(June-August 2018), and autumn (September-December 2018).

#### **AQMS** data

Hourly air pollutant concentrations in 25 AQMSs were downloaded from a website managed by the Korea Environment Corporation (http://www.airkorea.or.kr/ web). The AQMSs were equipped with national standard method monitors for five criteria pollutants. Hourly air pollutant concentrations were measured by automatic PM monitors based on the beta (β) attenuation method, a NO2 monitor based on the chemiluminescent method, a CO monitor based on the nondispersive infrared absorption method, and an O<sub>3</sub> monitor based on the ultraviolet photometric method. The detection limits of monitors at AQMSs were 5 μg/m<sup>3</sup> for  $PM_{2.5}$ , 10 µg/m<sup>3</sup> for  $PM_{10}$ , 0.1 ppb for  $NO_2$ , 0.05 ppm for CO, and 2 ppb for O<sub>3</sub>. Valid data were selected based on the national quality assurance/quality control (QA/ QC) operation guidelines published by the Korea Ministry of Environment (https://www.airkorea.or.kr/ web/board/3/267/?pMENU\_NO=145).

#### IMS data

In-situ measurements were performed on eight fixed monitoring sites within the test-bed area in Guro-gu, Seoul. A vehicle with standard method monitors used by the AQMSs was positioned at eight IMSs to obtain air pollutant concentrations. All IMS measurements strictly adhered to the installation and operation guidelines of the Korean Ministry of Environment and employed the same Korean Air Quality Monitoring Standard (KAMST) equipment used in Seoul's roadside AQMS network. Hourly concentrations of five air pollutants were measured

in each IMS for approximately 10 consecutive days in each season. The measurements were repeated for 12 weeks per season for four seasons at the eight IMSs. Detailed measurement schedules for the eight IMSs are provided in Table S2. QA/QC for measurements was conducted once per season for one week based on the national QA/QC operation guidelines published by the Korea Ministry of Environment (https://www.airkorea.or.kr/web/board/3/267/?pMENU\_NO=145).

#### **Spatial autocorrelation analysis**

Moran's index (Moran's *I*) was used as an indicator of spatial autocorrelation to identify the homogeneity and heterogeneity of air pollutants at different monitoring sites (Fang et al. 2015). Spatial autocorrelations were analyzed by the global index, which represented the overall spatial autocorrelation at all monitoring sites (Moran 1948), and the local index, which represented the local spatial autocorrelation at each specific monitoring site (Anselin 1995).

# Global spatial autocorrelation

Global Moran's I (GMI) was used to determine the overall spatial autocorrelation of air pollutant concentrations across the entire monitoring sites and ranged from -1 to 1; if GMI was > 0 (0 < GMI < 1), it represented a positive spatial autocorrelation. A larger GMI denoted that the area had a stronger spatial agglomeration with a similar concentration in the adjacent area. In contrast, if GMI was < 0 (-1 < GMI < 0), it represented a negative spatial autocorrelation, which was spatially dispersed and implied that the area had less spatial agglomeration with a different concentration in

the adjacent area. If GMI = 0, air pollutant concentrations were randomly distributed, and there was no spatial autocorrelation. GMI was calculated using eq (1):

$$GMI = \frac{\sum_{i=1}^{n} \sum_{j=1}^{n} w_{ij} (x_i - \bar{x}) (x_j - \bar{x})}{\frac{1}{n} \sum_{i=1}^{n} (x_i - \bar{x})^2 \sum_{i=1}^{n} \sum_{j=1}^{n} w_{ij}}$$
(1)

where n is the number of monitoring sites;  $x_i$  and  $x_j$  are air pollutant concentrations of spatial i and j monitoring sites, respectively;  $\bar{x}$  is the mean x; and  $w_{ij}$  is the spatial weight matrix that represents the spatial relationship between spatial i and j sites. If  $w_{ij}$  is 1, the spatial units i and j are adjacent; otherwise,  $w_{ij}$  is 0.

The Z values of the standardized statistic were used to test the significance of global spatial autocorrelations and calculated according to eqs (2), (3), and (4).

$$Z = \frac{I - E(I)}{\sqrt{V(I)}} \tag{2}$$

$$E(I) = -\frac{1}{n-1} \tag{3}$$

$$V(I) = E(I^{2}) - [E(I)]^{2}$$
(4)

where E(I) and V(I) are the expected values and variances of the Moran's I, respectively.

Among the above equations, the significance level of the global Moran's I can be measured by Z(I). At the 0.05 significance level, Z > 1.96 represents a positive spatial autocorrelation between spatial units, and -1.96 < Z < 1.96 indicates that the spatial autocorrelation is not obvious. If Z < -1.96, then a negative autocorrelation exists between spatial units, and the attribute value tends to be distributed.

# **Local spatial autocorrelation**

Local Moran's *I* (LMI) was used to determine the local spatial autocorrelation of air pollutant concentrations at each monitoring site. A high positive LMI implied that the concentrations were similar to those in the surrounding neighborhood; high-high clusters (i.e., high values in a high-value neighborhood) and low-low clusters (i.e., low values in a low-value neighborhood). Meanwhile, a high negative LMI implied that a spatial autocorrelation was obviously different from the concentrations at the surrounding monitoring sites; spatial outliers included high-low (i.e., a high value in a low-value neighborhood) and low-high (i.e., a low value in a high-value neighborhood) outliers. The LMI was calculated according to eq (5):

LMI = 
$$\frac{(x_i - \bar{x}) \sum_{j \neq i}^{n} w_{ij} (x_j - \bar{x})}{\frac{1}{n} \sum_{i=1}^{n} (x_i - \bar{x})^2}$$
 (5)

where n,  $x_i$ ,  $x_j$ ,  $\bar{x}$ , and  $w_{ij}$  are the same as the parameters for GMI.

The standardized statistic of LMI can also be measured by Z. At the 0.05 significance level, Z > 1.96 shows that sites with high concentrations were surrounded by sites with high concentrations (i.e., high–high) and that sites with low concentrations were surrounded by sites with low concentrations (low–low). In contrast, Z < -1.96 shows that sites with high concentrations were surrounded by sites with low concentrations (high–low) and that sites with low concentrations were surrounded by sites with high concentrations were surrounded by sites with high concentrations (low–high). When Z = 0, air pollutant concentrations were randomly distributed. When -1.96 < Z < 1.96, the spatial autocorrelation was not significant.

# Statistical analysis

All calculations and statistical analyses were conducted using R software (version 4.4.3). Air pollutant concentrations at monitoring sites were compared by season to determine significant differences in means using one-way analysis of variance (ANOVA) and Tukey's post-hoc tests. Results with p-value < 0.05 was considered to indicate statistical significance for two-sided statistical tests. Pearson correlation coefficients (r) between air pollutants in AQMSs and IMSs were calculated using Pearson correlation analysis. The correlations were classified into three categories: weak, moderate, and strong correlations. The absolute value of the coefficient (|r|) ranged from 0–0.3 for weak correlations, 0.3-0.6 for moderate correlations, and 0.6-1.0 for strong correlations. Spatial autocorrelation analyses using GMI and LMI were conducted using the moran.test() and localmoran() function in the package "spdep" (Bivand et al. 2025) of R software.

In the box plots, mean and median values were represented by a dotted line and a plain line, respectively. Box limits represented the 25th and 75th percentiles, and the whiskers extended to the 10th and 90th percentiles. Circles above the 90th percentile represented the 95th percentile, and circles below the 10th percentile represented the 5th percentile. Box plots were drawn using SigmaPlot 10.0 (Systat Software, San Jose, CA, U.S.A.).

#### Results

# Seasonal characteristics of air pollutants

The hourly concentrations of five air pollutants in 25 AQMSs, one AQMS, and eight IMSs in four seasons are

shown in Figure 2. The average hourly concentrations among the monitoring sites were significantly different across the four seasons (p < 0.01). The hourly air pollutant concentrations at the 25 AQMSs were significantly different among the four seasons (p < 0.001). The highest PM<sub>2.5</sub>, PM<sub>10</sub>, NO<sub>2</sub>, and CO concentrations at the 25 AQMSs were observed in the winter, whereas the lowest concentrations were observed in the summer. Conversely, the highest O<sub>3</sub> concentrations at the 25 AQMSs were recorded in the summer, whereas the lowest concentrations were noted in the winter. Hourly air pollutant concentrations at IMSs were significantly different in the four seasons (p < 0.001), and the seasonal characteristics of air pollutants at IMSs were similar to those at the 25 AQMSs.

The hourly mean PM<sub>2.5</sub> concentrations in the summer and autumn at the IMSs were significantly higher than those at the 25 AQMSs (p < 0.001), whereas the hourly mean PM<sub>2.5</sub> concentrations in the spring at the IMSs and 25 AQMSs differed slightly (p = 0.07). The hourly mean PM<sub>10</sub> concentrations across four seasons at the IMSs were significantly higher than those at the 25 AQMSs (p <0.001). The hourly mean NO<sub>2</sub> concentrations in the winter, spring, and summer at the IMSs were significantly higher than those at the 25 AQMSs (p < 0.05). The hourly mean CO concentrations in four seasons at the IMSs were significantly higher than those at the 25 AQMS (p <0.001). However, the hourly mean O<sub>3</sub> concentrations in the spring and summer at the IMSs were significantly lower than those at the 25 AQMSs (p < 0.001). Descriptive statistics of hourly mean air pollutant concentrations at one AQMS and the IMSs in Guro-gu are shown in Tables S3–S7. The hourly mean air pollutant concentrations at the AQMS and IMSs in Guro-gu were significantly different in all seasons (p < 0.05).

The noncompliance rates of the Korean air quality standards (KAAQSs) of air pollutants at AQMSs and IMSs are shown in Table 1. The noncompliance rates for the PM<sub>2.5</sub> KAAQS (with a 24-hr mean of 35  $\mu$ g/m³) were approximately 30% in the winter and spring at all sites. The PM<sub>10</sub> KAAQS did not exceed the 24-hr mean of 100  $\mu$ g/m³ in the summer at any site. The NO<sub>2</sub> and CO concentrations in the 25 AQMSs and IMSs in all seasons did not exceed the KAAQSs. Noncompliance rates for the PM<sub>10</sub> KAAQS at the IMSs were higher than at the 25 AQMSs in the winter, spring, and autumn, whereas noncompliance rates for the O<sub>3</sub> KAAQS at the IMSs in the summer were lower than at the 25 AQMSs.

# Seasonal correlations between air pollutants

Seasonal correlations between air pollutants at the 25 AQMSs and the IMSs are shown in Table 2. The seasonal correlation analysis was conducted to examine how the spatial relationships of pollutant concentrations vary across the four seasons and between monitoring network scales. The PM concentrations in the AQMSs and the IMSs showed significant positive correlations with NO<sub>2</sub> and CO, especially in the winter and autumn (r values > 0.5). PM<sub>2.5</sub> concentrations in AQMSs and the IMSs showed strong positive correlations with

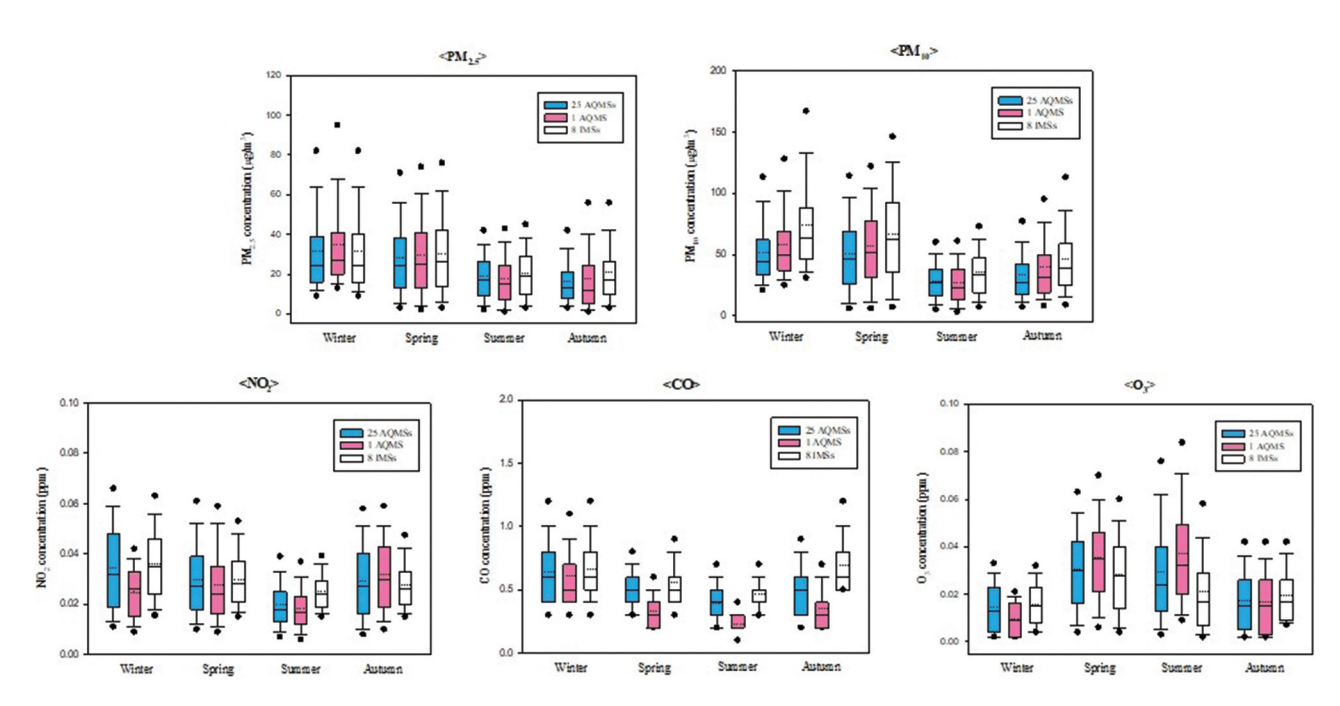


Figure 2. Hourly concentrations of air pollutants at 25 air quality monitoring stations (AQMSs) (blue), one AQMS in Guro-gu (pink), and eight in-situ monitoring sites (IMSs) in Guro-gu (white).

Table 1. The noncompliance rates (%) of the Korean ambient air quality standards (KAAQSs) of air pollutants by season. AQMS – air quality monitoring station, IMS – in-situ monitoring station.

Air pollutant	Site	Winter	Spring	Summer	Autumn
PM <sub>2.5</sub> (24-h)	25 AQMSs	32.5	27.3	6.6	7.1
$(35  \mu g/m^3)$	Guro AQMS	35.1	33.8	5.8	12.5
	IMSs	31.7	34.1	4.3	12.5
PM <sub>10</sub> (24-h)	25 AQMSs	5.9	7.0	0	3.2
$(100  \mu g/m^3)$	Guro AQMS	9.3	10.4	0	4.2
	IMSs	20.7	12.2	0	5.6
O <sub>3</sub> (8-h)	25 AQMSs	0	3.1	6.1	0
(0.06 ppm)	Guro AQMS	0	7.3	12.1	0
	IMSs	0	3.4	2.0	0
O <sub>3</sub> (1-h)	25 AQMSs	0	0.3	1.7	0
(0.1 ppm)	Guro AQMS	0	0.6	2.5	0
	IMSs	0	0.2	0.3	0

Table 2. Pearson correlation coefficients (r values) among five air pollutants in 25 air quality monitoring stations (AQMSs) in Seoul (gray) and eight in-situ monitoring sites (IMSs) in Guro-gu, Seoul (white) by season.

	PM <sub>2.5</sub>	PM <sub>10</sub>	$NO_2$	CO	03	PM <sub>2.5</sub>	PM <sub>10</sub>	NO <sub>2</sub>	CO	03
			Winter					Spring		
PM <sub>2.5</sub>	1	0.91**	0.57**	0.63**	-0.34**	1	0.78**	0.47**	0.62**	-0.003
$PM_{10}$	0.94**	1	0.48**	0.57**	-0.24**	0.77**	1	0.39**	0.49**	0.10*
$NO_2$	0.55**	0.49**	1	0.78**	-0.78**	0.16*	0.18**	1	0.66**	-0.50**
CO	0.58**	0.57**	0.63**	1	-0.57**	0.35**	0.34**	-0.43**	1	-0.32**
03	-0.06*	-0.03	-0.63**	-0.26**	1	0.04	0.11*	-0.55**	-0.29**	1
			Summer					Autumn		
PM <sub>2.5</sub>	1	0.94**	0.41**	0.37**	0.35**	1	0.76**	0.64**	0.66**	-0.28**
$PM_{10}$	0.90**	1	0.42**	0.38**	0.36**	0.79**	1	0.48**	0.45**	-0.22**
$NO_2$	0.32**	0.37**	1	0.40**	-0.08*	0.61**	0.48**	1	0.71**	-0.65**
CO	0.16*	0.21**	0.33**	1	0.01	0.63**	0.50**	0.76**	1	-0.49**
0 <sub>3</sub>	0.27**	0.30**	-0.04	0.03	1	-0.22**	-0.21**	-0.50**	-0.44**	1

<sup>\*\*</sup>Estimates are statistically significant at p < 0.001.

Table 3. Global spatial autocorrelations of air pollutants at the 25 air quality monitoring stations (AQMSs) and eight in-situ monitoring sites (IMSs) over four seasons. GMI – global Moran's index.

	City-scale at 25 AQMSs				Small-scale at 8 IMSs			
GMI	Winter	Spring	Summer	Autumn	Winter	Spring	Summer	Autumn
PM <sub>2,5</sub>	0.02	0.03	0.06	0.23*	-0.01	-0.30	-0.29	-0.33
$PM_{10}$	-0.18	-0.26	0.02	0.13	-0.07	-0.32	-0.29	-0.15
$NO_2$	-0.17	-0.04	0.12	0.01	0.01	-0.35	-0.20	-0.12
CO	0.09	-0.18	-0.16	0.07	-0.36	0.16	-0.12	-0.35
03	0.27*	0.09	0.13	0.21*	-0.11	0.21*	-0.19	0.19*

<sup>\*</sup>Estimates are statistically significant at p < 0.05.

 $NO_2$  and CO concentrations in autumn (*r* values > 0.6). However, O<sub>3</sub> at the IMSs had significant negative weak correlations with PM in the winter and autumn, whereas positive correlations were observed in the summer. Strong negative correlations between O<sub>3</sub> and NO<sub>2</sub> were observed in the winter, whereas weak correlations were observed in the summer. In the winter, the correlation between O<sub>3</sub> and PM concentrations at the AQMS sites was nearly random, with coefficients close to zero, whereas the IMS sites showed stronger negative correlations, with coefficients ranging from -0.2 to -0.3. This finding demonstrates that the strength and nature of inter-pollutant relationships can vary substantially depending on the monitoring scale.

#### Spatial autocorrelations by area scale

Global spatial autocorrelations at the 25 AQMSs (cityscale) and eight IMSs (small-scale) are shown in Table 3 using GMI. Significant global spatial homogeneity of PM<sub>2.5</sub> at the 25 AQMSs was observed in the autumn, with a positive GMI (p < 0.05). However, PM<sub>2.5</sub> concentrations in the winter and spring at the 25 AQMSs were randomly distributed with a GMI of approximately 0. PM<sub>10</sub> concentrations in the winter and spring at the 25 AQMSs were spatially dispersed with a negative GMI. O<sub>3</sub> concentrations in the winter and autumn at the 25 AQMSs were spatially agglomerated with a significant positive GMI (p < 0.05). Local spatial autocorrelations at

<sup>\*</sup>Estimates are statistically significant at p < 0.05.

each AQMS in Seoul are shown in Tables S8-S12 using LMI.

 $PM_{2.5}$  and  $PM_{10}$  at the IMSs across all seasons had negative GMI, indicating that they were spatially dispersed.  $PM_{2.5}$ ,  $PM_{10}$ , and  $NO_2$  concentrations in the winter at the IMSs were randomly distributed, with a GMI of approximately 0.  $PM_{10}$  concentrations in the winter and spring at the IMSs were spatially dispersed, with a negative GMI.  $O_3$  concentrations in the spring and autumn at the IMSs were spatially agglomerated, with a significant positive GMI (p < 0.05).  $NO_2$  and CO concentrations in the summer and autumn at the IMSs were spatially distributed, with a negative GMI.

The local spatial autocorrelations at the eight IMSs are shown in Figure 3. Patterns of the local spatial autocorrelation at each monitoring site differed by season.  $PM_{2.5}$  concentrations at locations 3, 5, and 8 were spatially dispersed in the winter, with a negative GMI, whereas they were spatially agglomerated in the summer and autumn, with a positive GMI.  $PM_{10}$  concentrations at location 3 and 8 were spatially dispersed in the winter, with a negative GMI, whereas they were randomly distributed in the autumn, with a GMI of approximately 0.  $O_3$  concentrations at location 7 were spatially agglomerated in all seasons.

# **Discussion**

In this study, small-scale monitoring was conducted using the same standard instruments as those employed

in the government-managed AQMS to ensure data accuracy and enable direct comparison between AQMS and IMS measurements. Although low-cost sensors can provide practical and cost-effective alternatives for air quality assessment, their accuracy is generally lower than that of reference methods (Shin et al. 2024). By employing national reference instruments managed by the Seoul Metropolitan Government Research Institute of Public Health and Environment, measurement uncertainty was minimized and data harmonization between AQMS and IMS was secured. To capture fine-scale spatial variability of roadside air pollution, the Ministry of Environment has previously employed vehicles equipped with reference instruments for real-time monitoring (Kim et al. 2015). Similarly, in this study, a monitoring vehicle equipped with standard instruments was stationed at eight sites within a 1 km<sup>2</sup> test area, providing high-resolution air quality data that complemented the AQMS observations. This complementarity underscores the value of integrating AQMS data, which provide long-term continuity suitable for evaluating temporal trends and health impacts, with IMS data, which offer high spatial resolution essential for identifying localized variations and sources. Such a dual-use approach ultimately enhances the accuracy of exposure assessments and improves the reliability of epidemiological findings.

There were distinct seasonal patterns of air pollutant concentrations. High PM concentrations were observed in the winter, followed by spring. High PM concentrations in Korea have typically been observed in the winter and spring (Kim et al. 2020), which is consistent with

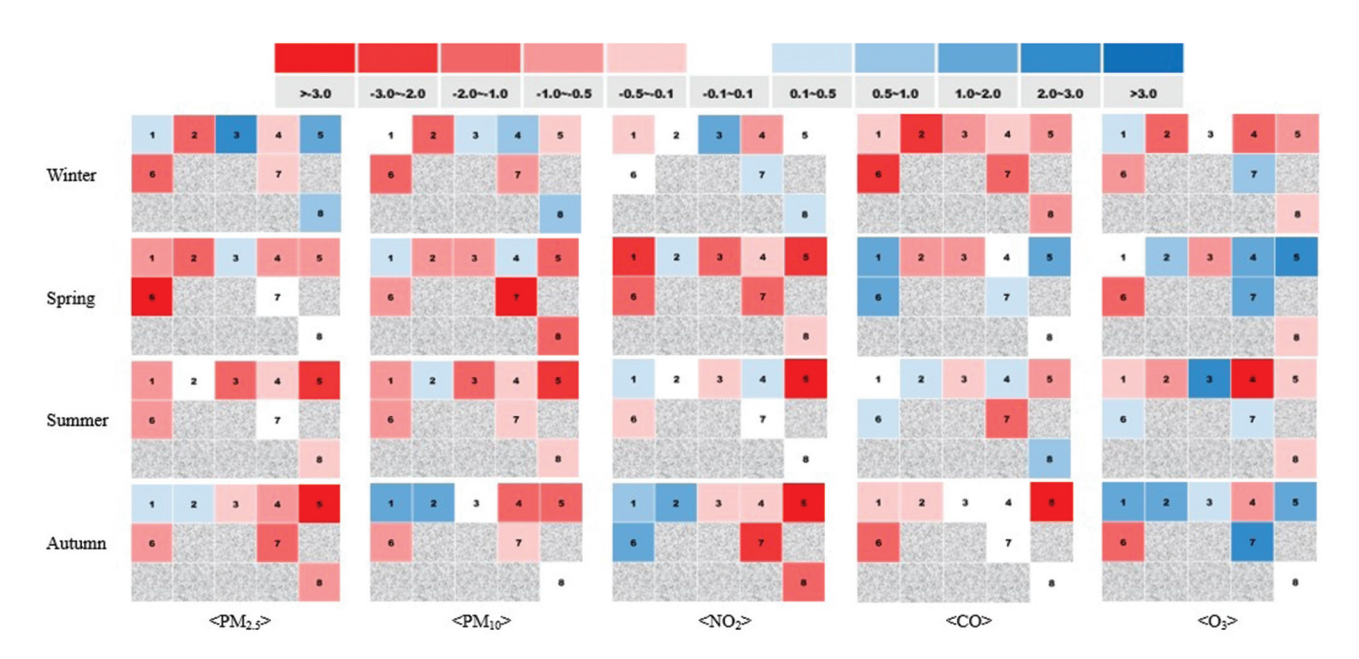


Figure 3. Local Moran's I (LMI) values of air pollutants in eight in-situ monitoring sites (IMSs) by season. Blue denotes a positive spatial autocorrelation, red denotes a negative spatial autocorrelation, and white denotes no spatial autocorrelation.

the seasonal variation observed in the present study. Such air quality is affected by the long-range transport of air pollutants from East Asia, regional sources, and meteorological conditions in the Korean Peninsula (Kim et al. 2018). Meanwhile, low PM concentrations were observed in the summer, when the PM concentrations were reduced by a washout effect during the rainy season, along with rapid air dispersion (Kim and Kim 2000).

Noncompliance rates of the KAAQS of PM<sub>2.5</sub> at AQMSs and IMSs were > 30% in the winter and the spring. A PM<sub>2.5</sub> advisory in Seoul, Korea, was issued 10 times (winter: seven times, spring: twice, and autumn: once) during the sampling periods. In a PM<sub>2.5</sub> advisory, personal exposure to PM<sub>2.5</sub> was affected by high outdoor PM<sub>2.5</sub> concentration due to high PM<sub>2.5</sub> infiltration (Guak and Lee 2018). PM<sub>2.5</sub> persisted in ambient air for a long period due to the low temperature, reduced wind speed, and less air circulation in the winter (Li et al. 2021). Therefore, the seasonal trend of ambient PM<sub>2.5</sub> levels should be considered when making policies to reduce personal exposure to air pollution.

High  $O_3$  concentrations were observed in the spring and summer, whereas low O<sub>3</sub> concentrations occurred in the winter. O<sub>3</sub> is generated by a photochemical reaction with O<sub>3</sub> precursors (oxides of nitrogen [NO<sub>x</sub>] and volatile organic compounds [VOCs]). O<sub>3</sub> concentrations were affected by meteorological conditions due to higher air temperature and intense solar irradiation, which trigger photochemical reactions with O<sub>3</sub> precursors (NO<sub>x</sub> and VOCs) in the spring and summer more so than in the winter (Hwang and Park 2019; Ribas and Peñuelas 2004). On the other hand, during the winter, the rate of photochemical reactions with O<sub>3</sub> was slow due to the NO<sub>x</sub> titration effect (Jhun et al. 2015). In other studies in Korea, O<sub>3</sub> levels in the spring and summer were significantly higher than those in the winter (Hwang and Park 2019; Vellingiri et al. 2015). These results are consistent with those in China (Chen et al. 2017) and Turkey (Kasparoglu, Incecik, and Topcu 2018).

High NO<sub>2</sub> and CO concentrations were observed in the winter and autumn, and low NO<sub>2</sub> concentrations occurred in the summer and spring. The hourly mean NO<sub>2</sub> and CO concentrations in AQMSs and IMSs did not exceed the corresponding KAAQS. The highest NO<sub>2</sub> concentration can be explained by the weak solar irradiation available for photochemical conversion to O<sub>3</sub>, along with stagnant atmosphere conditions (Li et al. 2012). In contrast, intense light irradiation also caused low concentrations of NO<sub>2</sub> and other nitrogen oxides (Marković et al. 2008). NO<sub>2</sub> is a gaseous pollutant with motor vehicle emissions as a main source (Costa et al.

2017). CO is a colorless, nonirritating, odorless, and tasteless gas generated by the incomplete combustion of carbon compounds such as burning gasoline, wood, propane, charcoal, or other fuel (Sørhaug et al. 2006).

AQMS data in one administrative district of Seoul (Guro-gu) were significantly different from IMS data surrounding the AQMS. The hourly mean PM and NO<sub>2</sub> concentrations at the IMSs were generally higher than those at the Guro AQMS. Especially, hourly mean CO concentrations in four seasons at the IMSs were approximately two-fold higher than at the AQMS. High CO concentrations were mainly due to on-road vehicle emissions (Ghaffarpasand et al. 2020). However, the O<sub>3</sub> concentrations at the IMSs in the spring and summer were significantly lower than those at the Guro AQMS. The rate of exceeding the KAAQS for O<sub>3</sub> at the Guro AQMS in the summer was more than twofold higher than that at the IMSs, which may have been affected by the characteristics of the monitoring location; the IMSs were located near streets and parking lots, whereas the Guro AQMS was located on a building rooftop. A study found that the O<sub>3</sub> concentrations on a rooftop were higher than those on the street level (Park et al. 2015; Väkevä et al. 1999). In addition, each IMS was likely influenced by emission sources specific to its geographic characteristics, which may have contributed to the relatively higher concentrations observed compared to the AQMS.

The correlations between air pollutants differed by season. Stronger positive correlations between PM<sub>2.5</sub> and gaseous pollutants (e.g., NO<sub>2</sub> and CO) were observed in the autumn than in other seasons. This result implied that increases in NO2 and CO concentration affected PM<sub>2.5</sub> concentrations in the autumn. High correlations between PM and gaseous pollutants in the autumn were observed in China (Li et al. 2017); the results were similar to those obtained in the present study, with low PM concentration in the autumn. However, O<sub>3</sub> had weaker correlations with PM in the winter and spring compared to the correlations in the summer. As mentioned above, this was mainly associated with the photochemical reactions as properties of O<sub>3</sub> related to climate and meteorological conditions (Ribas and Peñuelas 2004). PM pollution was severe in the winter and spring, whereas it was mild in the summer. In the winter and spring, there was low temperature and weak light intensity, which resulted in fewer reactions between PM and O<sub>3</sub>. In the summer, high temperatures and strong light intensity lead to an increase in O<sub>3</sub> concentration due to increase photochemical reactions. Thus, seasonal characteristics between PM and O<sub>3</sub> need to be considered on taking preventive control policies of air pollution.

This study observed significant seasonal variations and correlations in air pollutant concentrations across different spatial scales over the course of one year. Air pollutant concentrations are a critical input for population exposure modeling. However, previous studies have often relied on city-scale data from AQMSs as surrogate measures for exposure, highlighting the need for improvements in precision and accuracy (Guak et al. 2021). Compared with AQMSs, which primarily measure urban background concentrations, reflecting the seasonal and spatial variability of air pollutants more closely related to actual living environments can enhance the accuracy of exposure modeling. Given that spatiotemporal variability can substantially influence the outcomes of exposure models, future studies should prioritize providing finer-scale monitoring data to improve the reliability and robustness of exposure assessments.

In this study, the Moran Index was applied as a method to assess spatial autocorrelation by evaluating the degree of similarity between a given region and its neighboring areas. Global spatial autocorrelation can be used to identify whether the overall sampling areas have spatial autocorrelations, and, if so, to reflect the correlation intensity. In the 25 AQMSs in Seoul, GMIs of PM<sub>2.5</sub> and O<sub>3</sub> were close to zero in the spring and were significantly positive in the autumn. This result implies a random distribution in the spring and spatial agglomeration in the autumn, possibly related to seasonal patterns of PM<sub>2.5</sub> and O<sub>3</sub> concentrations. Low PM<sub>2.5</sub> and O<sub>3</sub> concentrations were observed in the autumn, whereas high PM<sub>2.5</sub> and O<sub>3</sub> concentrations were noted in the spring. Spatial autocorrelation was affected by seasonal patterns of air pollutants (Zhou et al. 2021).

Global spatial autocorrelation patterns of PM<sub>2.5</sub> were different at the city-scale in 25 gu of Seoul and smallscale areas of 1 km<sup>2</sup> in Guro-gu, Seoul. Global autocorrelations of PM<sub>2.5</sub> in all seasons were spatially homogenized with positive GMIs at the 25 AQMSs. However, global spatial autocorrelations of PM<sub>2.5</sub> in all seasons were spatially dispersed with negative GMIs at the IMSs. AQMS data at the city-scale were limited to represent air quality in smaller areas, including unmonitored locations. Hence, spatial autocorrelation should be considered at a smaller scale than the city-scale.

Seasonal local spatial patterns of homogeneity and heterogeneity of air pollutants were differently observed in a spatial smaller scale using local spatial autocorrelation. It was difficult to generalize and identify the local spatial autocorrelation patterns of air quality in each monitoring area. Various spatial variations could be affected by significant complex factors, depending on local emission sources, climate conditions, or meteorological occurrences, such as

local circulations and topographic features (Wang et al. 2014). Air pollutant concentrations were spatially heterogeneous in areas with different emission sources and varying air pollutant dispersion characteristics (Valari et al. 2020). Various spatial autocorrelations in different areas have been reported in other studies (Shen et al. 2019; Wang et al. 2015; Xu et al. 2019).

For future population exposure assessments, when applying pollutant concentrations derived from small grid units (e.g., 1 km<sup>2</sup>) that account for spatial autocorrelation identified in this study, it is important to interpret the results not only in terms of spatial structure but also in relation to the characteristics of the exposed population. For example, population density, age distribution, and time-activity patterns within each grid may influence actual exposure levels, even if surrounding concentrations are spatially correlated. A previous study demonstrated that considering both pollutant concentrations and population density can improve the accuracy of population-level exposure assessments (Woo et al. 2022). Therefore, when grid-based pollutant concentrations are used in exposure research, integrating demographic and behavioral factors into the interpretation of spatial autocorrelation results may provide a more comprehensive understanding of population exposure disparities.

The limitations of this study were several. Although the eight grids were selected based on the urban AQMS in Guro-gu, the testbed configuration was centered on the AQMS and thus spatially concentrated in the eastern part of the district. However, each IMS was located in a site with distinct geographic characteristics, allowing us to reflect environmental heterogeneity despite the spatial concentration. Moreover, because the IMS sites were placed closer to human activity zones—such as roadside environments—they were able to capture finer high-resolution pollution patterns that the rooftop-located AQMS might not fully detect. Full trajectory-based exposure tracking (e.g., using personal GPS or wearable sensors) provides the most accurate assessment, but it is often infeasible in large population studies due to privacy, cost, and logistical constraints. In this context, highresolution ambient monitoring offers a practical compromise, enabling refined exposure estimates at the population level and reducing misclassification in spatially heterogeneous areas. This study is an important step toward improving area-level exposure estimation. Future studies could build upon this framework by integrating spatial concentration data with personal movement patterns or indoor exposure models to construct more comprehensive exposure profiles.

#### **Conclusion**

Seasonal spatial variations of five air pollutants were identified in city-scale and small-scale areas in Seoul using measurements with standard monitoring methods over one year. Seasonal spatial autocorrelations of air pollutant concentrations at the 25 AQMSs in the city-scale were different from those in smaller-scale (1 km<sup>2</sup>) areas that were obtained from the eight IMSs. Seasonal patterns of spatial autocorrelation for air pollutants at the city-scale did not reflect small-scale variations. These findings highlight the limitations of relying solely on AQMS data for exposure assessment and underscore the value of high-resolution data to reduce estimation errors. This study offers a framework for improving air quality management and exposure assessment strategies by accounting for spatial-temporal variations, especially in areas lacking dense monitoring networks. Therefore, our findings provide evidence that seasonal spatial variations of air pollutants at a small scale should be considered to assess more accurate estimations of personal exposure to air pollutants with implications for human health.

# **Acknowledgment**

The authors acknowledge the time and effort invested by all the study participants.

#### **Disclosure statement**

No potential conflict of interest was reported by the author(s).

# **Funding**

The authors acknowledge financial support from the Korea Environmental Industry & Technology Institute (KEITI) through the Core Technology Development Project for Environmental Disease Prevention and Management funded by the Korea Ministry of Environment (MOE) [grant number RS-2021-KE001337] and by the Basic Science Research Program through the National Research Foundation of Korea (NRF) funded by the Ministry of Education [grant number RS-2023-00275753].

#### **About the authors**

**Sooyoung Guak** is a Research Professor in the Department of Environmental Health Sciences at Seoul National University, South Korea.

**Jaehoon An** is a researcher in the Department of Health Sciences at Seoul National University, South Korea.

**Dong-Hyun Lee** is a researcher in Consulting & Technology for Environment Health Safety, South Korea.

Wonho Yang is a Professor in the Department of Occupational Health at Daegu Catholic University, South Korea

**Jusung Park** is a Dean in Seoul Metropolitan Government Research Institute of Public Health and Environment, South Korea

**Kiyoung Lee** is a Professor in the Department of Environmental Health Sciences at Seoul National University, South Korea.

# **Data availability statement**

All original data used in this study are available upon request.

#### References

Anselin, L. 1995. Local indicators of spatial association— LISA. *Geogr. Anal* 27 (2):93–115. doi: 10.1111/j.1538-4632.1995.tb00338.x.

Arunachalam, S., A. Valencia, Y. Akita, M.L. Serre, M. Omary, V. Garcia, and V. Isakov. 2014. A method for estimating urban background concentrations in support of hybrid air pollution modeling for environmental health studies. *Int. J. Environ. Res. Public. Health* 11 (10):10518–36. doi: 10. 3390/ijerph111010518.

Atkinson, R.W., I.M. Carey, A.J. Kent, T.P. van Staa, H. R. Anderson, and D.G. Cook. 2013. Long-term exposure to outdoor air pollution and incidence of cardiovascular diseases. *Epidemiology* 24 (1):44–53. doi: 10.1097/EDE. 0b013e318276ccb8.

Bivand, R., M. Altman, L. Anselin, R. Assuncao, O. Berke, G. Blanchet, and D. Yu. 2025. Spdep: Spatial dependence, weighting schemes. Statistics. R Package Version 1.1-7. https://cran.r-project.org/web/packages/spdep/spdep.pdf.

Chen, C., J. Cai, C. Wang, J. Shi, R. Chen, C. Yang, H. Li, Z. Lin, X. Meng, A. Zhao, et al. 2018. Estimation of personal PM<sub>2.5</sub> and BC exposure by a modeling approach – results of a panel study in Shanghai, China. *Environ. Int* 118:194–202. doi: 10.1016/j.envint.2018.05.050.

Chen, W., H. Tang, and H. Zhao. 2015. Diurnal, weekly and monthly spatial variations of air pollutants and air quality of Beijing. *Atmos Environ*. 119:21–34. doi: 10.1016/j.atmo senv.2015.08.040.

Chen, Y., L. Zang, J. Chen, D. Xu, D. Yao, and M. Zhao. 2017. Characteristics of ambient ozone (O<sub>3</sub>) pollution and health risks in Zhejiang Province. *Environ. Sci. Pollut. Res. Int.* 24 (35):27436–44. doi: 10.1007/s11356-017-0339-x.

Cohen, A.J., M. Brauer, R. Burnett, H.R. Anderson, J. Frostad, K. Estep, K. Balakrishnan, B. Brunekreef, L. Dandona, R. Dandona, et al. 2017. Estimates and 25-year trends of the global burden of disease attributable to ambient air pollution: An analysis of data from the global burden of diseases study 2015. *Lancet* 389 (10082):1907–18. doi: 10. 1016/S0140-6736(17)30505-6.

Costa, A.F., G. Hoek, B. Brunekreef, and A.C.M. Ponce de Leon. 2017. Effects of NO<sub>2</sub> exposure on daily mortality in

- São Paulo, Brazil. *Environ. Res.* 159:539–44. doi: 10.1016/j. envres.2017.08.041.
- Dėdelė, A., and A. Miškinytė. 2019. Seasonal and site-specific variation in particulate matter pollution in Lithuania. *Atmos. Pollut. Res.* 10 (3):768–75. doi: 10.1016/j.apr.2018. 12.004.
- Dong, Z., H. Wang, P. Yin, L. Wang, R. Chen, W. Fan, Y. Xu, and M. Zhou. 2020. Time-weighted average of fine particulate matter exposure and cause-specific mortality in China: A nationwide analysis. *Lancet Planet. Health* 4 (8): e343–51. doi: 10.1016/S2542-5196(20)30164-9.
- Fang, C., H. Liu, G. Li, D. Sun, and Z. Miao. 2015. Estimating the impact of urbanization on air quality in China using spatial regression models. *Sustainability* 7 (11):15570–92. doi: 10.3390/su71115570.
- Ghaffarpasand, O., M.R. Talaie, H. Ahmadikia, A.T. Khozani, and M.D. Shalamzari. 2020. A high-resolution spatial and temporal on-road vehicle emission inventory in an Iranian metropolitan area, Isfahan, based on detailed hourly traffic data. *Atmos. Pollut. Res.* 11 (9):1598–609. doi: 10.1016/j. apr.2020.06.006.
- Guak, S., and K. Lee. 2018. Different relationships between personal exposure and ambient concentration by particle size. *Environ. Sci. Pollut. Res. Int.* 25 (17):16945–50. doi: 10. 1007/s11356-018-1889-2.
- Guak, S., S.-G. Lee, J. An, H. Lee, and K. Lee. 2021. A model for population exposure to PM<sub>2.5</sub>: Identification of determinants for high population exposure in Seoul. *Environ. Pollut* 285:117406. doi: 10.1016/j.envpol.2021.117406.
- Hoek, G., R. Beelen, K. de Hoogh, D. Vienneau, J. Gulliver, P. Fischer, and D. Briggs. 2008. A review of land-use regression models to assess spatial variation of outdoor air pollution. *Atmos Environ*. 42 (33):7561–78. doi: 10.1016/j. atmosenv.2008.05.057.
- Hu, J., Y. Wang, Q. Ying, and H. Zhang. 2014. Spatial and temporal variability of PM<sub>2.5</sub> and PM<sub>10</sub> over the North China Plain and the Yangtze River Delta, China. *Atmos Environ*. 95:598–609. doi: 10.1016/j.atmosenv.2014.07.019.
- Hwang, S.H., and D.U. Park. 2019. Ambient endotoxin and chemical pollutant (PM<sub>10</sub>, PM<sub>2.5</sub>, and O<sub>3</sub>) levels in South Korea. *Aerosol. Air Qual. Res* 19 (4):786–93. doi: 10.4209/aaqr.2018.06.0235.
- Jhun, I., B.A. Coull, A. Zanobetti, and P. Koutrakis. 2015. The impact of nitrogen oxides concentration decreases on ozone trends in the USA. *Air Qual. Atmos Health* 8 (3):283–92. doi: 10.1007/s11869-014-0279-2.
- Ji, W., Y. Wang, and D. Zhuang. 2019. Spatial distribution differences in PM<sub>2.5</sub> concentration between heating and non-heating seasons in Beijing, China. *Environ. Pollut* 248:574–83. doi: 10.1016/j.envpol.2019.01.002.
- Kasparoglu, S., S. Incecik, and S. Topcu. 2018. Spatial and temporal variation of O<sub>3</sub>, NO and NO<sub>2</sub> concentrations at rural and urban sites in Marmara region of Turkey. *Atmos. Pollut. Res.* 9 (6):1009–20. doi: 10.1016/j.apr.2018.03.005.
- Kim, B., and D. Kim. 2000. Studies on the environmental behaviors of ambient PM<sub>2.5</sub> and PM<sub>10</sub> in Suwon area. *J. Korean Soc. Atmos. Environ* 16:89–101.
- Kim, D., H.E. Choi, W.M. Gal, and S. Seo. 2020. Five year trends of particulate matter concentrations in Korean regions (2015–2019): When to ventilate? *Int. J. Environ. Res. Public. Health* 17 (16):5764. doi: 10.3390/ijerph17165764.

- Kim, K.H., D. Woo, S.-B. Lee, and G.-N. Bae. 2015. On-road measurements of Ultrafine particles and associated air pollutants in a densely populated area of Seoul, Korea. *Aerosol. Air Qual. Res* 15 (1):142–53. doi: 10.4209/aaqr.2014.01.0014.
- Kim, Y., J. Seo, J.Y. Kim, J.Y. Lee, H. Kim, and B.M. Kim. 2018. Characterization of PM<sub>2.5</sub> and identification of transported secondary and biomass burning contribution in Seoul, Korea. *Environ. Sci. Pollut. Res. Int.* 25 (5):4330–43. doi: 10.1007/s11356-017-0772-x.
- Li, J., W. Gao, L. Cao, L. He, X. Zhang, Y. Yan, J. Mao, J. Xin, L. Wang, G. Tang, et al. 2021. Effects of different stagnant meteorological conditions on aerosol chemistry and regional transport changes in Beijing, China. *Atmos Environ*. 258:118483. doi: 10.1016/j.atmosenv.2021.118483.
- Li, K.H., W. Song, X.J. Liu, J.L. Shen, X.S. Luo, X.Q. Sui, B. Liu, Y.K. Hu, P. Christie, and C.Y. Tian. 2012. Atmospheric reactive nitrogen concentrations at ten sites with contrasting land use in an arid region of Central Asia. *Biogeosciences* 9 (10):4013–21. doi: 10.5194/bg-9-4013-2012.
- Li, L., J. Qian, C.Q. Ou, Y.X. Zhou, C. Guo, and Y. Guo. 2014. Spatial and temporal analysis of air pollution index and its timescale-dependent relationship with meteorological factors in Guangzhou, China, 2001–2011. *Environ. Pollut* 190:75–81. doi: 10.1016/j.envpol.2014.03.020.
- Li, R., L. Cui, J. Li, A. Zhao, H. Fu, Y. Wu, L. Zhang, L. Kong, and J. Chen. 2017. Spatial and temporal variation of particulate matter and gaseous pollutants in China during 2014–2016. *Atmos Environ*. 161:235–46. doi: 10.1016/j. atmosenv.2017.05.008.
- Marković, D.M., D.A. Marković, A. Jovanović, L. Lazić, and Z. Mijić. 2008. Determination of O3, NO2, SO2, CO and PM<sub>10</sub> measured in Belgrade urban area. *Environ. Monit. Assess* 145 (1–3):349–59. doi: 10.1007/s10661-007-0044-1.
- Marshall, J.D., E. Nethery, and M. Brauer. 2008. Within-urban variability in ambient air pollution: Comparison of estimation methods. *Atmos Environ*. 42 (6):1359–69. doi: 10.1016/j.atmosenv.2007.08.012.
- Merbitz, H., S. Fritz, and C. Schneider. 2012. Mobile measurements and regression modeling of the spatial particulate matter variability in an urban area. *Sci. Total Environ*. 438:389–403. doi: 10.1016/j.scitotenv.2012.08.049.
- Mills, I.C., R.W. Atkinson, S. Kang, H. Walton, and H. R. Anderson. 2015. Quantitative systematic review of the associations between short-term exposure to nitrogen dioxide and mortality and hospital admissions. *BMJ Open* 5 (5): e006946. doi: 10.1136/bmjopen-2014-006946.
- Moran, P.A.P. 1948. The interpretation of statistical maps. *J. R. Stat. Soc. B* 10 (2):243–51. doi: 10.1111/j.2517-6161. 1948.tb00012.x.
- Park, S.-B., K.-H. Kwak, B.-S. Han, G. Ganbat, H. Lee, J.M. Seo, S.-H. Lee, and J.-J. Baik. 2015. Measurements of turbulent flow and ozone at rooftop and sidewalk sites in a high-rise building area. *Sola* 11 1–4. doi: 10.2151/sola.2015-001.
- Raja, N.B., O. Aydin, N. Türkoğlu, and İ. Çiçek. 2018. Characterising the seasonal variations and spatial distribution of ambient  $PM_{10}$  in urban Ankara, Turkey. *Environ. Process.* 5 (2):349–62. doi: 10.1007/s40710-018-0305-8.
- Ribas, À., and J. Peñuelas. 2004. Temporal patterns of surface ozone levels in different habitats of the North Western



- Mediterranean Basin. Atmos Environ. 38 (7):985-92. doi: 10.1016/j.atmosenv.2003.10.045.
- Shen, Y., L. Zhang, X. Fang, H. Ji, X. Li, and Z. Zhao. 2019. Spatiotemporal patterns of recent PM<sub>2.5</sub> concentrations over typical urban agglomerations in China. Sci. Total Environ. 655:13–26. doi: 10.1016/j.scitotenv.2018.11.105.
- Shin, J., J. Woo, Y. Choe, G. Min, D. Kim, D. Kim, S. Lee, and W. Yang. 2024. Spatiotemporal exposure assessment of PM<sub>2.5</sub> concentration using a sensor-based air monitoring System. Atmosphere 15 (6):664. doi: atmos15060664.
- Sørhaug, S., S. Steinshamn, O.G. Nilsen, and H.L. Waldum. 2006. Chronic inhalation of carbon monoxide: Effects on the respiratory and cardiovascular system at doses corresponding to tobacco smoking. *Toxicology* 228 (2–3):280–90. doi: 10.1016/j.tox.2006.09.008.
- Su, J.G., M. Jerrett, B. Beckerman, D. Verma, M.A. Arain, P. Kanaroglou, D. Stieb, M. Finkelstein, and J. Brook. 2010. A land use regression model for predicting ambient volatile organic compound concentrations in Toronto, Canada. Atmos Environ. 44 (29):3529–37. doi: 10.1016/j.atmosenv.
- Tessum, M.W., T. Larson, T.R. Gould, C.D. Simpson, M. G. Yost, and S. Vedal. 2018. Mobile and fixed-site measurements to identify spatial distributions of traffic-related pollution sources in los Angeles. Environ. Sci. Technol. 52 (5):2844-53. doi: 10.1021/acs.est.7b04889.
- Väkevä, M., K. Hämeri, M. Kulmala, R. Lahdes, J. Ruuskanen, and T. Laitinen. 1999. Street level versus rooftop concentrations of submicron aerosol particles and gaseous pollutants in an urban street canyon. Atmos Environ. 33 (9):1385–97. doi: 10.1016/S1352-2310(98)00349-5.
- Valari, M., K. Markakis, E. Powaga, B. Collignan, and O. Perrussel. 2020. EXPLUME v1.0: A model for personal exposure to ambient O<sub>3</sub> and PM<sub>2.5</sub>. Geosci. Model Dev. 13 (3):1075-94. doi: 10.5194/gmd-13-1075-2020.

- Vellingiri, K., K.-H. Kim, J.Y. Jeon, R.J.C. Brown, and M.-C. Jung. 2015. Changes in NO<sub>x</sub> and O<sub>3</sub> concentrations over a decade at a central urban area of Seoul, Korea. Atmos Environ. 112:116-25. doi: 10.1016/j.atmosenv.2015.04.032.
- Wang, Y., Q. Ying, J. Hu, and H. Zhang. 2014. Spatial and temporal variations of six criteria air pollutants in 31 provincial capital cities in China during 2013–2014. Environ. *Int* 73:413–22. doi: 10.1016/j.envint.2014.08.016.
- Wang, Y.Q., X.Y. Zhang, J.Y. Sun, X.C. Zhang, H.Z. Che, and Y. Li. 2015. Spatial and temporal variations of the concentrations of PM<sub>10</sub>, PM<sub>2.5</sub> and PM<sub>1</sub> in China. Atmos. Chem. Phys. 15 (23):13585-98. doi: 10.5194/acp-15-13585-2015.
- Woo, J., G. Min, D. Kim, M. Cho, K. Sung, J. Won, J. Lee, J. Shin, and W. Yang. 2022. Existing population exposure assessment using PM<sub>2.5</sub> concentration and the geographic information System. J. Environ. Health Sci 48 (6):298-305. doi: 10.5668/JEHS.2022.48.6.298.
- Xu, J., W. Yang, B. Han, M. Wang, Z. Wang, Z. Zhao, Z. Bai, and S. Vedal. 2019. An advanced spatio-temporal model for particulate matter and gaseous pollutants in Beijing, China. Atmos Environ. 211:120-27. doi: 10.1016/j.atmosenv.2019. 04.011.
- Yang, Y., and G. Christakos. 2015. Spatiotemporal characterization of ambient PM<sub>2.5</sub> concentrations in Shandong Province (China). Environ. Sci. Technol. 49 (22):13431-38. doi: 10.1021/acs.est.5b03614.
- Zhao, P.S., F. Dong, D. He, X.J. Zhao, X.L. Zhang, W. Z. Zhang, Q. Yao, and H.Y. Liu. 2013. Characteristics of concentrations and chemical compositions for PM<sub>2.5</sub> in the region of Beijing, Tianjin, and Hebei, China. Atmos. Chem. Phys. 13 (9):4631–44. doi: 10.5194/acp-13-4631-2013.
- Zhou, D., Z. Lin, L. Liu, and J. Qi. 2021. Spatial-temporal characteristics of urban air pollution in 337 Chinese cities and their influencing factors. Environ. Sci. Pollut. Res. Int. 28 (27):36234-58. doi: 10.1007/s11356-021-12825-w.